

ROCK MAGNETIC PROPERTIES OF A LOESS-PALEOSOLS COMPLEX FROM MIRCEA VODA (ROMANIA)

C. NECULA, C. PANAIOTU

University of Bucharest, Faculty of Physics, Bucharest – Magurele, Romania
E-mail: c3necula@yahoo.com

Received July 27, 2011

Abstract. Thermomagnetic curves, hysteresis parameters, isothermal and viscous remanence and FORC diagrams were performed for several representative loess and paleosol samples from Mircea Voda profile. The main magnetic mineral is magnetite with mixed grain size: dominant SP in paleosols and with significant MD contribution in loess.

Key words: loess-paleosol, rock-magnetic parameters, mineral magnetism, FORC.

1. INTRODUCTION

The wind-blown sediments from Romania successfully record the major paleoclimatic variations for the last approximately 600 ka. Loess deposits from Romania can be found on wide areas covering regions from Danube Plain, Dobrogea and Moldova. Usual stratigraphy is characterized by a section with consecutive loess and paleosol layers reflecting the succession between cold and dry climates during which dust were accumulated and warmer and more humid climatic regimes favourable to paleosols development. Two sequences of Romanian loess, both from South-Eastern Romania, were studied up to now: Mostistea located in the Danube Plain and Mircea Voda located in Dobrogea Plateau [1–7]. The results showed that magnetic susceptibility measured across the loess sections record with accuracy major climatic changes which took place during the late Quaternary period: paleosols are characterized by high values of magnetic susceptibility whereas loess units display weaker values. These variations are similar with those recorded in China, Central Asia and Europe proving that the main mechanism responsible with magnetic enhancement in paleosols is under the control of the same climatic oscillations covering wide regions from Northern Hemisphere mid latitudes. Furthermore the closely correlation between the low-field magnetic susceptibility and deep-sea isotopic oxygen records linked the Romanian loess magnetic variations to the major global climatic changes during

the Quaternary. In addition the correlation between the terrestrial and marine proxies allowed the establishment of a first chronology for Romanian loess confirmed by independent OSL and IRSL ages.

However detailed rock-magnetic properties and their relation with paleoclimate were investigated only for Mostistea loess sequence [1, 2]. We present here a first systematic, multi-parameter rock magnetic properties for Mircea Voda loess-paleosol complex located in the Dobrogea Plateau. This will contribute to a better understanding of the relationship between magnetic parameters and pedogenesis and will complete the information about paleoclimate evolution in Romania for the last 600 ka. For this purpose we present the results about magnetic mineralogy, concentration and domain state for five loess-paleosol couplets. In addition FORC (First Order Reversal Curve) analysis is performed on the loess-paleosol sequence providing high resolution information about the link between magnetic mineralogy, domain state and paleoclimate.

2. REGIONAL SETTINGS AND MEASUREMENTS

The new loess-paleosol deposit is localized near the Mircea Voda village in the Dobrogea (Dobrogea) Plateau, at about 15 km from the Danube River. The loess sequence comprises five well-developed paleosol (S1 to S5) with five intercalated loess layers (L1 to L5). The section has around 26 m thick with apparently no breaks or erosions [5]. [4] measured the magnetic susceptibility along the profile depth but with a very low resolution: at least 10 samples were taken for each of the younger paleosols and at least three samples for each of the older ones. Based on the magnetic susceptibility data they built a rough time scale for Mircea Voda loess section tuning the magnetic susceptibility data to various target proxies. They concluded that the paleosols were developed during the odd numbers of Marine Isotopic Stages whereas loess was accumulated during the MIS even numbers. A high resolution record of magnetic susceptibility was provided by [5] and a continuous time scale was built: the whole Mircea Voda section was sampled at 10 cm interval. Their results confirmed the ages obtained by [4] for Mircea Voda loess section. IRSL (Infrared Stimulated Luminescence) ages performed on feldspar grains from the first three loess layers by [7] support the accumulation of wind-blown dust during the glacial stages confirming thus the above chronologies. Also a broadly agreement was found between both time scales and the OSL (Optical Stimulated Luminescence) dating on silt quartz (4–11 μm) [5].

For this study all the measurements were performed on bulk material. We used the same laboratory techniques as in [8], magnetic measurements being focused on determination of hysteresis parameters, temperature-dependent susceptibility variations and FORC diagrams. All measurements were performed at

the Paleomagnetic Laboratory, University of Bucharest. Representative samples were selected from each loess and paleosols units. Hysteresis loops of the selected samples were measured using Princeton Measurements Corporation Vibrating Sample Magnetometer 3 900 in a maximum field of 500 mT. Hysteresis parameters (saturation magnetization, M_s , remanent magnetization, M_{rs} , and coercive force, H_c respectively) were determined after the correction for para- or diamagnetic contribution identified from the slope at high fields. Coercivity of remanence, H_{cr} , was obtained imparting an IRM in a field of 500 mT and then the samples were demagnetized in a stepwise backfield from 0 to -500 mT. Temperature-dependent magnetic susceptibility measurements were made using a KLY-3 Kappabridge with a CS3 high-temperature device heating the samples from room temperature to 700°C . To avoid possibly oxidation, the samples were heated and cooled in an argon atmosphere. The sample holder and thermocouple's contributions to susceptibility were then subtracted.

Saturation Isothermal Remanent Magnetization (SIRM) was induced using a Magnon International pulse magnetizer in a field of 2T. Also the remanence after the application of a reverse field of -0.3T was measured. All remanences were measured using a JR5 spinner magnetometer. The S ratio was calculated as $S_{-300\text{mT}} = S = \text{IRM}_{-300\text{mT}}/\text{IRM}_{2\text{T}}$.

Time dependent IRM measurements were conducted using the same Magnon International pulse magnetizer. Each sample acquired a SIRM in a 2T field and the remanence was measured immediately (after approximately 10 seconds) and re-measured after 900s. The viscous decay coefficient, normalized to SIRM was computed for each sample as $S_d = (\text{IRM}_{10\text{s}} - \text{IRM}_{900\text{s}}) / \log(900\text{s}/10\text{s})$ [9].

FORC analysis FORC measurements were conducted using the same PMC VSM 3900 magnetometer. To construct a FORC diagram, 111 first-order reversal curves were measured using a saturating field of 1T. The FORC data processing was performed using FORCinel software developed by [10]. The calculation of first-order reversal curve (FORC) diagrams use locally weighted regression smoothing and can perform an optimum smoothing factor calculation.

3. RESULTS AND DISCUSSIONS

3.1. MAGNETIC MINERALOGY

The first information about the magnetic mineralogy comes from the S ratio which measures the relative abundance variations of ferrimagnetic and antiferromagnetic minerals (*e.g.* [11, 12]). Both loess and paleosol layers show S ratios between 0.8 and 1 indicating that the magnetic mineralogy is dominated by low coercivity magnetic minerals (Fig. 1).

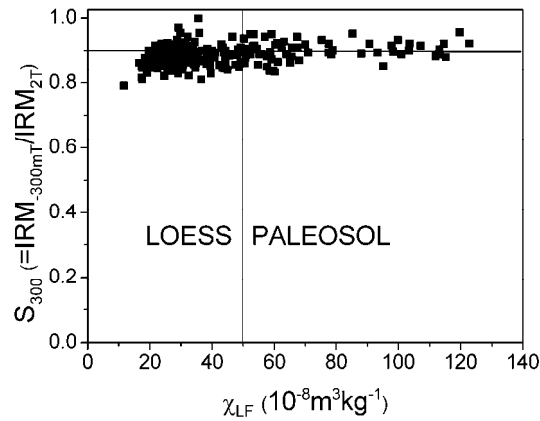


Fig.1 – S_{300} ratio ($=\text{IRM}_{300\text{mT}}/\text{IRM}_{2\text{T}}$) versus low field magnetic susceptibility.

Evidence that these magnetic minerals are magnetite and maghemite is provided by the temperature-dependent susceptibility variations (Fig. 2). All paleosol samples become paramagnetic at approximately 585°C, the Curie point of nearly stoichiometric magnetite (*e.g.* [8, 13, 14, 15]). The Curie points between 590 and 620°C highlighted by loess samples suggest the presence of partially oxidized magnetite [13]. Thus magnetite is the major contributor to the magnetic susceptibility in both loess and paleosol units. The steady increase of magnetic susceptibility up to 200°C in paleosol samples is usually attributed to the gradual unblocking of fine ferromagnetic particles (near the superparamagnetic/single domain boundary) (*e.g.* [14, 15]) suggesting that paleosols contain more fine-grained particles probably of pedogenic origin. Except S_0 paleosol, all loess and paleosol samples exhibit wide maxima between 150 and 300°C which could be due to reduction of hematite to magnetite when heating organic matter in samples, or from the neoformation of minor ferrimagnetic phases during heating ([16]).

S_0 and L5 units present further drop of magnetic susceptibility between 300 and 450°C which is commonly interpreted as the conversion of ferrimagnetic maghemite to weakly magnetic hematite ([14, 15, 16; 17]). Furthermore [17] proved that usually fine grained maghemite is transformed to hematite between 300 and 450°C. This susceptibility drop is more prominent in S_0 than in L5 indicating that paleosol can contain finer grained pedogenic maghemite grains. Both S_0 and L5 highlight significant peaks in the heating curves at approximately 510°C. All other loess and paleosol layers do not display such a behavior. In addition this characteristic cannot be seen in the cooling curves (not shown) suggesting that this is not a Hopkinson peak but rather is due to the neo-formation of magnetite grains from iron-containing silicates/clays [14, 16] or due to the formation of magnetite by reduction due to the burning of organic matter [18].

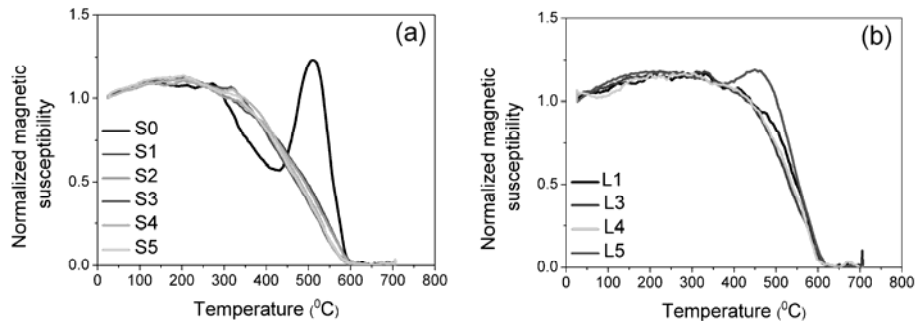


Fig. 2 –Temperature-dependent magnetic susceptibility curves for representative samples of: a) paleosol; b) loess. The magnetic susceptibility was normalized to room temperature.

3.2. MAGNETIC GRANULOMETRY

Viscous decay of SIRM provides the highest resolution indication for relative abundance of SP grains [9, 19]. Table 1 displays the calculated values of viscous decay coefficient, S_d [9], for several representative samples from each Mircea Voda loess and paleosol unit. After 900s paleosol samples present a one order of magnitude higher remanence viscous relaxation than loess units. This suggests that paleosols from Mircea Voda loess section contain a high amount of superparamagnetic magnetic minerals, in concordance with the results from Mostistea loess section [2].

Table 1

Viscous decay coefficient for several representative samples from Mircea Voda loess profile

Unit	IRM(t_0) [A/m]	IRM(t) [A/m] (after 900s)	S _d	S _d /SIRM (%)
S1	2.56215	2.41633	0.07461	2.91215
L2	1.96848	1.95598	0.0064	0.32489
S2	3.52035	3.27038	0.12791	3.63342
L3	2.43716	2.41633	0.01066	0.43735
S4	4.62436	4.16609	0.2345	5.07097
L4	1.63936	1.63519	0.00213	0.13004

Hysteresis loops are widely used as rapid indicators of coercivity spectrum and domain state of magnetic minerals (Fig. 3). All of the hysteresis curves are closed below 300 mT which suggest the dominance of soft magnetic minerals (magnetite and maghemite) [15, 16]. However the loops of the loess samples systematically closed to higher fields than the paleosols samples. This can be evidence that the most effective carriers of remanence loess are single-domain (SD) and/or pseudosingle-domain (PSD) magnetite grains [16]. Another explanation is that loess contains a significantly higher amount of antiferromagnetic minerals.

However neither SIRM nor the temperature-dependent susceptibility confirms the presence of the hard magnetic phase. The paleosols hysteresis loops are steeper and thinner than the loess ones. Thus pedogenesis leads to a decrease of coercive force, H_c , and a corresponding increase in remanent saturation magnetization, M_s . Moreover hysteresis loops of paleosol samples shows a slight constriction in the middle section presenting the so called wasp-waisted shape. This suggests either the presence of a mixed SP-SD population or could reflect a contribution from the antiferromagnetic phase [20, 21, 22]. However the hard magnetic phase, if exists, has a very low contribution to the magnetic susceptibility. This result is thus consistent with the previous ones suggesting that production of soils is very favorable to the formation of an excess of ultrafine soft magnetic minerals.

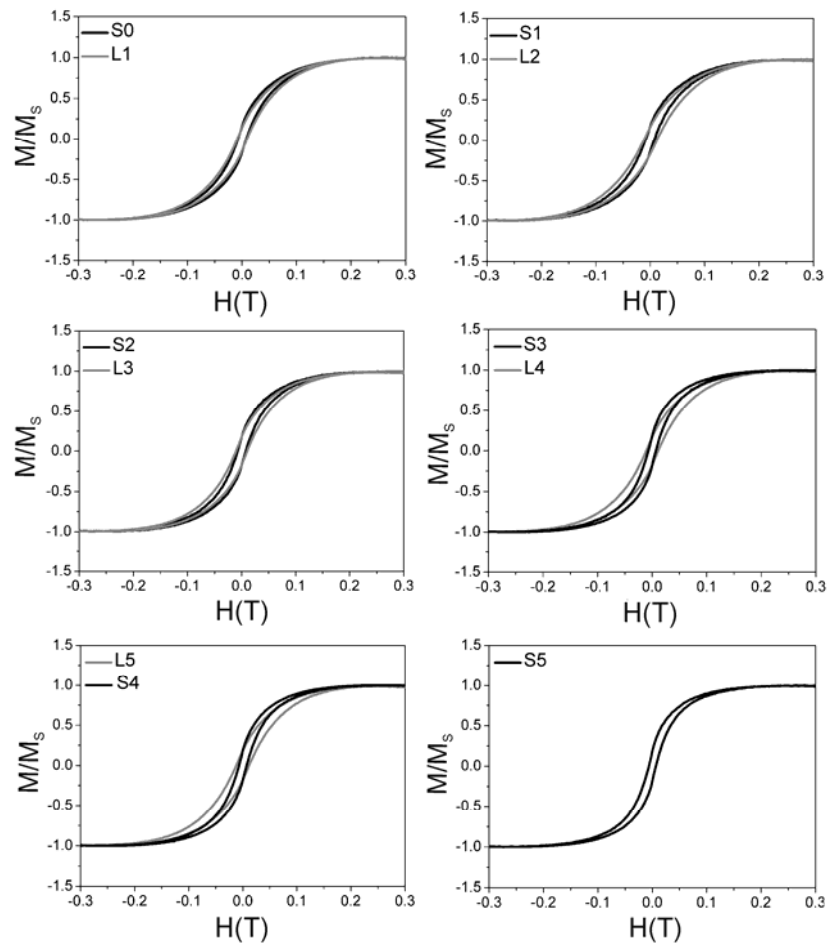


Fig. 3 – Hysteresis loops for representative samples from Mircea Voda loess section. All curves are corrected for para- and diamagnetic contributions.

Day diagram (M_{rs}/M_s versus H_{cr}/H_c) provides information about domain state of magnetic minerals [23, 24, 25]. The average magnetic grain size lies in the PSD region for both loess and paleosols (Fig. 4). The non-linear mixing curves of [25] are followed as an aid to a better interpretation of our data. Thus both loess and paleosols parallel more or less the SD-MD mixing curve 3 being moved towards SD-SP (10 nm) mixing curve. The deviation from the magnetite PSD model curves could be due to either a mixture of SP+SD grains or a mixture of SD+MD grains [25]. The general distribution of magnetic grain size at Mircea Voda is consistent with the results found for both Mostistea loess section ([2]) and Chinese Loess Plateau [15, 16, 25]: both loess and paleosols are formed from a heterogeneous mixture with a wide range of magnetic particle size [25, 26]. The Day diagram is not able to explain the significant contribution of pedogenic SP particles to the magnetic enhancement proved by the viscous decay experiments.

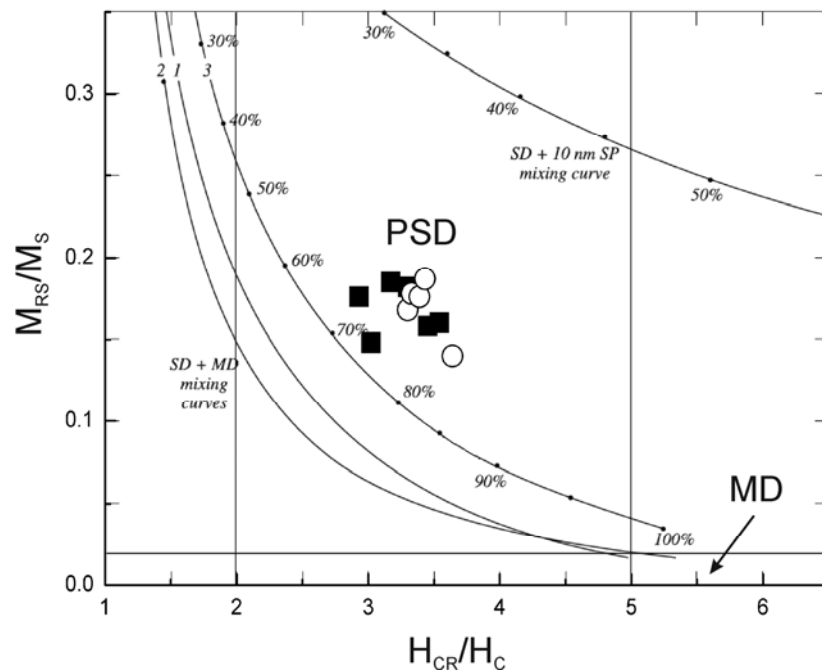


Fig. 4 – Hysteresis ratios plotted on a Day diagram of the loess and paleosol samples of the Mircea Voda section. Open circles represents loess samples and full squared represent paleosol samples. Theoretical mixing curves of Dunlop (2002a, b) are also plotted.

First-order reversal curve (FORC) diagrams are a standard technique widely used to characterize magnetic grain assemblages. They are able to provide high resolution information about composition, domain state and magnetostatic interactions [26, 27, 28, 29].

The two paleosol samples investigated show a FORC distribution with two peaks (Fig. 5). The first, highlighted by the small open contours located just near the origin of the FORC diagram (H_c well below 10 mT) indicate that the distribution have been shifted to lower coercivities by thermal relaxation effects. This represents the characteristic behavior of superparamagnetic particles [28, 30]. The vertical contours immediately adjacent to the H_u axis in the lower half plane come to confirm once more that the first peak represents undoubtedly the contribution of superparamagnetic particles to the FORC distribution [28]. The presence of superparamagnetic particles in paleosol samples is also confirmed by viscous decay of SIRM measurements. The secondary peak concentrated along the H_c axis (at $H_u = 0$) represent the signature of non-interacting SD particles [26, 28, 29]. If magnetostatic interactions would be present this central peak would have much vertical spread. This is consistent with the results of [26] and [31] which found that pedogenic magnetite is not affected by strong magnetostatic interactions. The distribution is displaced to lower coercivities (the peak is at approximately 10 mT) indicating that magnetic properties of paleosols are dominated by superparamagnetic particles. The amount of spreading along the H_c axis is a measure of the MD contribution to the sample [32]. Little divergence of outer contours of the S3 paleosol indicates a very small contribution from the MD and/or PSD grains to the magnetic properties of this sample. On the other hand recent soil (S0) show more pronounced divergent contours that intersect the H_u axis suggesting a much higher contribution of the MD and or/PSD grains to the total magnetization. The oldest paleosol presents also higher magnetic susceptibility values than the Holocene soil suggesting that this paleosol period was developed during more humid and warmer climatic conditions. This feature is characteristic to the whole Carpatho-Danubian-Black Sea area [1]. The results provided by FORC diagrams indicate thus that the magnetic enhancement in the oldest paleosol are due to the increase in concentration of superparamagnetic minerals as a result of more humid a warmer climate.

FORC distributions of the L3 loess sample show very similar behavior to S0 soil: a central peak representing the non-interacting SD particles signature and a secondary peak centered at the origin of the FORC diagram – a manifestation of SP grains. The presence of superparamagnetic component in loess samples suggest that loess in Mircea Voda might be affected by pedogenesis. However vertical contours in the lower left-hand portion of the FORC diagram that lie nearly parallel on the H_u axis are missing from the loess FORC diagram. This suggests that superparamagnetic influence is diminished in loess. In addition loess sample show much more divergent behavior of the outermost contours at low coercivities suggesting that the contribution of MD and or/PSD grains become much more important [31]. Moreover FORC distribution of the L2 loess sample show only a central peak with significant divergent contours that intersect H_u axis suggesting a mixture between non-interacting SD particles and MD and/or pseudo SD grains [8, 28]. These results are consistent with the time-dependent SIRM measurements which indicate much lower values of viscous decay coefficient in loess.

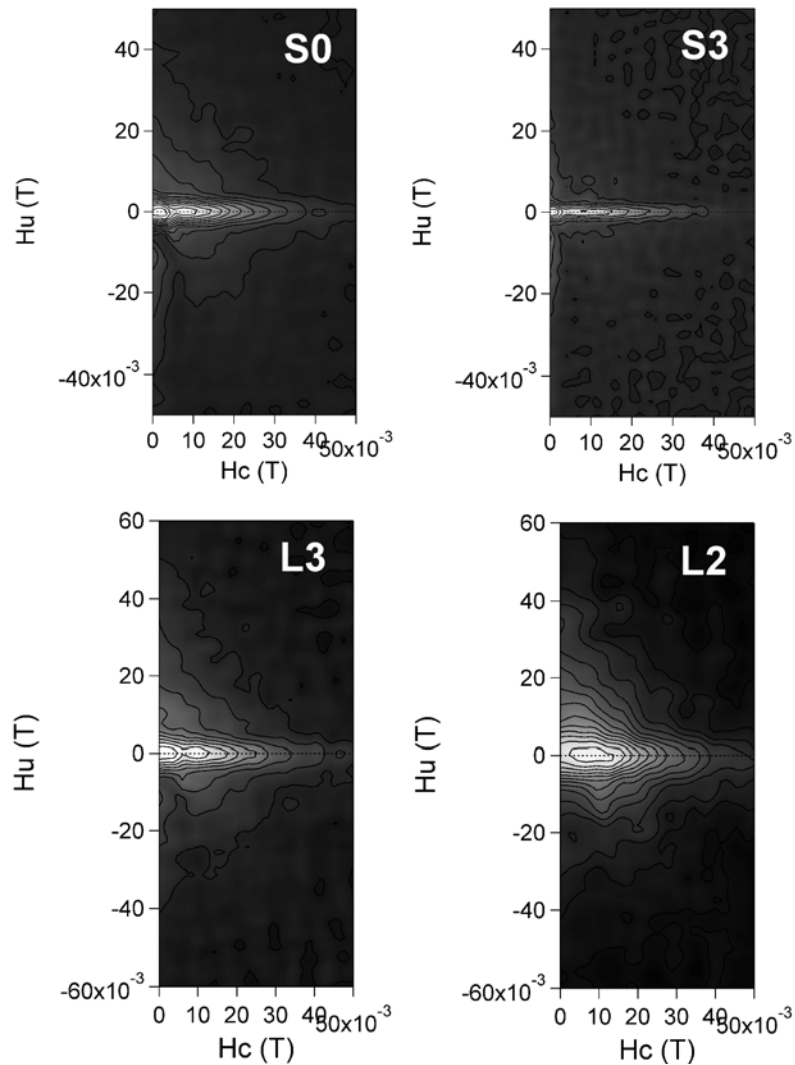


Fig. 5 – FORC diagrams for representative samples from Mircea Voda loess-paleosol complex.

Using the FORC results the ambiguity of the Day diagram can be now explained. Both loess and paleosols present complex magnetic phases. Superparamagnetic and non-interacting SD behavior is dominant in paleosols although a small contribution from MD and or/PSD can be visible. On the other hand loess sample is dominated by larger magnetic grains but with additional contribution from SD and SP particles. The Day diagram failed to unravel this complex magnetic signal, and thus the loess and paleosols samples may not be suitable for presentation on a Day plot [28].

4. CONCLUSIONS

Detailed rock-magnetic evidence for Mircea Voda loess-paleosol complex showed a uniform magnetic mineralogy along the whole loess profiles dominated by magnetite. Hysteresis properties and FORC distribution revealed a complex distribution of grain size magnetite. Using FORC diagrams, the contribution of different magnetic components in loess and paleosol samples was established. Thus FORC distribution showed different magnetic signature for loess and paleosols. Paleosols are dominated by superparamagnetic and non-interacting particles with less contribution from MD and/or PSD whereas loess samples are dominated by larger particles but also with important contribution from non-interacting SD and SP magnetic grains. These results are consistent with those obtained from loess deposits located in China, Central Asia and Europe proving that pedogenesis is favourable to the formation of new, ultrafine magnetic minerals.

Acknowledgements. Necula Cristian was supported by the strategic grant POSDRU/89/1.5/S/58852, Project „Postdoctoral programme for training scientific researchers” cofinanced by the European Social Found within the Sectorial Operational Program Human Resources Development 2007 – 2013. Magnetic measurements are a contribution from CNCSIS grant ID-31/2010.

REFERENCES

1. Panaiotu, C.G., Panaiotu, E.C., Grama, A., Necula, C., *Paleoclimatic record from a loess-paleosol profile in Southeastern Romania*, Phys. Chem. Earth (A), **26**, 11–12, 893–898 (2001).
2. C. Necula, C. Panaiotu, C.E. Panaiotu, A. Grama, *Magnetic properties of a loess-paleosol sequence at Mostiștea (Romania)*, Romanian Reports in Physics, **57**, 3, 453–46 (2005).
3. Necula C., C. Panaiotu, *Application of dynamic programming to the dating of a loess-paleosol sequence*, Romanian Reports in Physics, **60**, 1 (2008).
4. Buggle, Björn, Ulrich Hambach, Bruno Glaser, Natalia Gerasimenko, Slobodan Marković, Irina Glaser, Ludwig Zöller, *Stratigraphy and spatial and temporal paleoclimatic trends in Southeastern/Eastern European loess–paleosol sequences*, Quaternary International, **196**, 86–106 (2009).
5. Timar, A., D. Vandenberghe, E.C. Panaiotu, C.G. Panaiotu, C. Necula, C. Cosma, P. van den haute, *Optical dating of Romanian loess using fine-grained quartz*, Quaternary Geochronology, **5**, 2–3, 143–148 (2010).
6. Vasiliniuc, S., Timar Gabor, A., Vandenberghe, D.A.G., Panaiotu, C.G., Begy, R.C.S. and Cosma, C., *A high resolution optical dating study of the Mostiștea loess-paleosol sequence (SE Romania) using sand-sized quartz*, Geochronometria; doi 10.2478/s13386-011-0007-8, 2010.
7. Balescu Sanda, Michel Lamothe, Cristina Panaiotu, Cristian Panaiotu, *La chronologie IRSL des séquences loessiques de l'est de la Roumanie*, Quaternaire, **21**, 2, 115–126 (2010).
8. C. Panaiotu, C. Necula, T. Merezeanu, A. Panaiotu, C. Corban, *Anisotropy of magnetic susceptibility of Quaternary lava flows from the East Carpathians*, Romanian Reports in Physics, **63**, 2, 526–534 (2011).
9. Worm, H-U., *Time dependent IRM: A new technique for magnetic granulometry*, Geophysical Research Letters, **16**, 2557–2560 (1999).

10. R. J. Harrison & J. M. Feinberg, FORCinel: *An improved algorithm for calculating first-order reversal curve distributions using locally weighted regression smoothing*, *Geochem. Geophys. Geosyst.*, **9**, Q05016; doi:10.1029/2008GC001987, 2008.
11. Liu, Q., Roberts, A.P., Torrent, J., Horng, C.-S. & Larrasoana, J.C., *What do the HIRM and S-ratio really measure in environmental magnetism?*, *Geophys. Geochem. Geosyst.*, **8**; doi:10.1029/2007GC001717, 2007.
12. D. Heslop, *On the statistical analysis of the rock magnetic S-ratio*, *Geophys. J. Int.*, **178**, 159–161 (2009).
13. Diana Jordanova, Jozef Hus, and Raoul Geeraerts, *Palaeoclimatic implications of the magnetic record from loess/paleosol sequence Viatovo (NE Bulgaria)*, *Geophys. J. Int.*, **171**, 1036–1047 (2007).
14. Deng, C.L., *Paleomagnetic and mineral magnetic investigation of the Baicaoyuan loess–paleosol sequence of the western Chinese Loess Plateau over the last glacial– interglacial cycle and its geological implications*, *Geochemistry, Geophysics, Geosystems*, **9**, 4, Q04034; doi:10.1029/2007GC001928, 2008.
15. Chunsheng Jin, Qingsong Liu, *Revisiting the stratigraphic position of the Matuyama–Brunhes geomagnetic polarity boundary in Chinese loess*, *Palaeogeography, Palaeoclimatology, Palaeoecology*, **299**, 309–317 (2011).
16. Deng, C., R. Zhu, K. L. Verosub, M. J. Singer, and N. J. Vidic, *Mineral magnetic properties of loess/paleosol couplets of the central loess plateau of China over the last 1.2 Myr*, *J. Geophys. Res.*, **109**, B01103; doi:10.1029/2003JB002532, 2004.
17. Liu, Q., J. Torrent, B. A. Maher, Y. Yu, C. Deng, R. Zhu, and X. Zhao, *Quantifying grain size distribution of pedogenic magnetic particles in Chinese loess and its significance for pedogenesis*, *J. Geophys. Res.*, **110**, B11102; doi:10.1029/2005JB003726, 2005.
18. Liu, Q. S., C. L. Deng, Y. Yu, J. Torrent, M. J. Jackson, S. K. Banerjee, and R. X. Zhu, *Temperature dependence of magnetic susceptibility in argon environment: Implications for pedogenesis of Chinese loess/paleosols*, *Geophys. J. Int.*, **161**, 102–112; doi:10.1111/j.1365-246X.2005.02564.x., 2005.
19. Christoph E. Geiss and C. William Zanner, *How abundant is pedogenic magnetite? Abundance and grain size estimates for loessic soils based on rock magnetic analyses*, *Journal of Geophysical Research*, **111**, B12S21; doi:10.1029/2006JB004564, 2006.
20. Roberts, A.P., Cui, Y.L., Verosub, K.L., *Wasp-waisted hysteresis loops: Mineral magnetic characteristics and discrimination of components in mixed magnetic systems*, *Journal of Geophysical Research*, **100**, B9, 17909–17924 (1995).
21. Tauxe, L., Mullender, T.A.T., and Pick, T., *Potbellies, wasp-waists and superparamagnetism in magnetic hysteresis*, *Jour. Geophys. Res.*, **101**, 571–583 (1996).
22. Fabian, K., *Some additional parameters to estimate domain state from isothermal magnetization measurements*, *Earth Planet. Sci. Lett.*, **213**, 337–345 (2003).
23. Day, R., M. Fuller, and V. A. Schmidt, *Hysteresis properties of titanomagnetites: Grain-size and compositional dependence*, *Phys. Earth Planet. Inter.*, **13**, 260–267 (1977).
24. Dunlop, D.J., *Theory and application of the Day plot (Mrs/Ms versus Hcr/Hc) 1. Theoretical curves and tests using titanomagnetite data*, *Journal of Geophysical Research*, **107**, B3, 2056; doi:10.1029/2001JB000486, 2002.
25. Dunlop, D.J., *Theory and application of the Day plot (Mrs/Ms vs. Hcr/Hc) 2. Application to data for rocks, sediments and soils*, *J. Geophys. Res.*, **107**, B3, EPM 5-1 to 5-15; doi: 10.1029/2001JB000487, 2002.
26. Christoph E. Geiss, Ramon Egli, and C. William Zanner, *Direct estimates of pedogenic magnetite as a tool to reconstruct past climates from buried soils*, *Journal of Geophysical Research*, **113**, B11102; doi:10.1029/2008JB005669, 2008.
27. Pike, C. R., A. P. Roberts, and K. L. Verosub, *Characterizing interactions in fine magnetic particle systems using first order reversal curves*, *J. Appl. Phys.*, **85**, 6660–6667; doi:10.1063/1.370176, 1999.

28. Roberts, A. P., C. R. Pike, and K. L. Verosub, *First-order reversal curve diagrams: A new tool for characterizing the magnetic properties of natural samples*, *J. Geophys. Res.*, **105**, 28, 461–28,475; doi:10.1029/2000JB900326, 2000.
29. Ramon Egli, Amy P. Chen, and Michael Winklhofer, Kenneth P. Kodama, Chorng-Shern Horng, *Detection of noninteracting single domain particles using first-order reversal curve diagrams*, *Geochem. Geophys. Geosyst.*, Q01Z11; doi:10.1029/2009GC002916, 2010.
30. Pike, C. R., A. P. Roberts, and K. L. Verosub, *FORC diagrams and thermal relaxation effects in magnetic particles*, *Geophys. J. Int.*, **145**, 721–730 (2001).
31. I. H. M. van Oorschot, M. J. Dekkers and P. Havlicek, *Selective dissolution of magnetic iron oxides with the acid-ammonium-oxalate/ferrous-iron extraction technique—II. Natural loess and palaeosol samples*, *Geophys. J. Int.*, **149**, 106–117 (2002).
32. Pike, C. R., A. P. Roberts, M. J. Dekkers, and K. L. Verosub, *An investigation of multi-domain hysteresis mechanisms using FORC diagrams*, *Phys. Earth Planet. Inter.*, **126**, 11–25 (2001).